Evaluating the Stability of the Jianchuan Ancient Town with TerraSAR-X images

Xinning Gao [1], Menghua Li [1], Mengshi Yang [2], Li Tang [3], Bo-Hui Tang [1]

[1] Faculty of Land Resources Engineering, Kunming University of Science and Technology, Kunming, PR China - menghuali@kust.edu.cn
[2] School of Earth Sciences, Yunnan University, Kunming, PR China - yangms@ynu.edu.cn
[3] Faculty of Architecture and City Planning, Kunming University of Science and Technology, Kunming, PR China - 475583861@qq.com

Keywords: InSAR, Architectural Heritage, Deformation, Buildings stability assessment.

Abstract

Architectural heritage holds significant historical and cultural value. However, it faces substantial risks of deterioration stemming from natural aging and human activities. Traditional methods rely on manual surveys or ground-based measurements, which are time-consuming and labor-intensive, making it challenging to meet the demand for large-scale stability assessments of architectural heritage. In this study, we designed a methodology based on the analysis of differential deformation and angular distortion of buildings using InSAR line-of-sight (LOS) displacements. Then, the stability of buildings is categorized into three groups: stable, moderate, and unstable, using these stability indicators. A total of 74 TerraSAR-X images acquired from August 2017 to November 2019 in ascending orbit were used to monitor the Jianchuan Ancient Town, which has a history of over 650 years. Our evaluation reveals that among the 1891 architectures in Jianchuan Ancient Town, 1191 are rated as stable, 696 as moderate, and 4 as unstable. Time-series results indicate that one of the four unstable buildings exhibited a severe accelerating trend that requires attention. In conclusion, this methodology can enhance the capability to assess the stability of large-scale architectural heritages.

1. Introduction

Architectural heritage is experiencing challenges due to the increasing human activities and natural aging (Chen et al., 2021). These impacts expose the heritage to the inevitable threat of structural damage and collapse (Chen et al., 2023). In particular, deformation is generally divided into rapid deformation and slow deformation, where rapid deformation is caused by natural disasters such as geological hazards and floods, and slow deformation is caused by building aging and the combined effects of nature and man (Zhou et al., 2015). Therefore, it is crucial to monitor abnormal deformations dynamically and evaluate the stability of architectural heritage.

Traditional methods largely rely on manual surveys or ground-based measurements, which are time-consuming and labor-intensive, making it difficult to meet the demand for large-scale stability assessments of architectural heritage (Tang et al., 2016). However, the advancement in remote sensing, specifically the ongoing improvement of Synthetic Aperture Radar (SAR) and its algorithms, offers a new method for evaluating the stability of architectural heritage (Cigna et al., 2023; Tapete and Cigna, 2017). In particular, spaceborne SAR remote sensing, which does not require the prior installation of monitoring instruments in the building structure, can realise wide-range and high-density identification of subtle deformation of the heritage, having the advantages of non-destructive of structure and cost-saving (Chen et al., 2017; Du et al., 2024). During the past decade, InSAR also achieved progress in monitoring the architectural heritage, such as the Summer Palace in China (Tang et al., 2016), the historic buildings of Como in Italy (Nappo et al., 2021), Angkor Wat in Cambodia (Chen et al., 2019), and the Pagoda of Bagan in Myanmar (Chen et al., 2022).

In monitoring the stability of individual building at the large scale, the InSAR technology is used to estimate the deformation velocity and its time series of the building surface (Peduto et al., 2017; Waning, 2014). Then, based on the InSAR deformation results, structural health assessment indicators applicable to buildings are inversely performed. For instance, building damage induced by landslide movements and urbanization is assessed by combining angular distortion with maximum deformation (Bianchini et al., 2015). The risk level classification of buildings in the Kowloon district of Hong Kong and the Futian district of Shenzhen is based on the maximum deformation velocity and angular distortion (Ma et al., 2022).

In this study, we concentrate on evaluating the stability of architectural heritage structures and the effectiveness of such assessments when utilizing Interferometric Synthetic Aperture Radar (InSAR) technology. Jianchuan Ancient Town is located in Dali, China, where over 90% of the buildings were built before 1960. To evaluate the architectural heritages of Jianchuan Ancient Town, we designed a methodology based on the analysis of differential deformation and angular distortion of buildings using InSAR line-of-sight (LOS) displacements.

2. Study area and dataset

2.1 Jianchuan Ancient Town and its architectural heritages

Jianchuan Ancient Town is located in Dali, China, which is the major trading and military hub on the Southern Silk Road, as well as the Tea-Horse Ancient Road (Figure 1). Over 90% of the buildings in the ancient town are historic buildings built before 1960, including the Ximen Street Ancient Architecture Complex, a collection of Yuan, Ming, and Qing buildings, which has been listed as the sixth batch of national key protected cultural relics units of China. Unlike other ancient cities, in Jianchuan Ancient Town, many architectural relics and historic buildings have been preserved for residential use, and

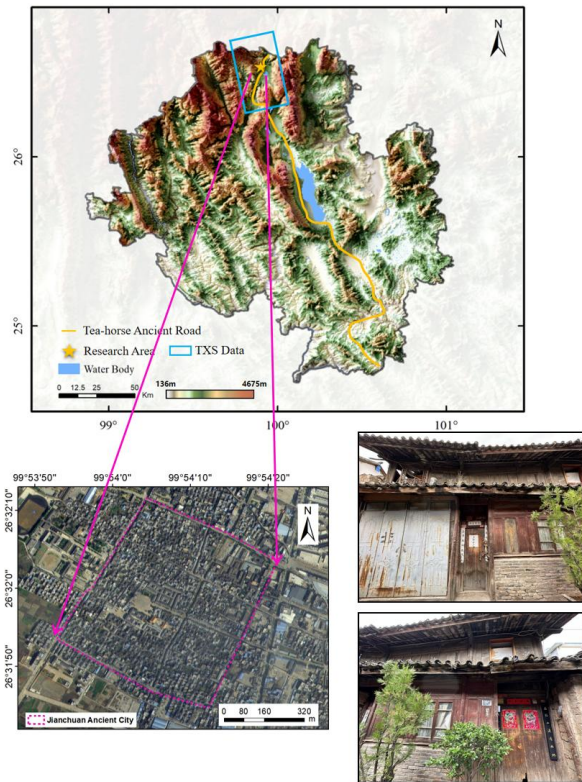historic buildings are interspersed with modern ones, forming a mix of the old and new buildings.

Figure 1. Location of Jianchuan Ancient Town. On the lower right is the satellite image of the Jianchuan Ancient Town. On the lower left are photos of the architectural heritages of the Jianchuan Ancient Town.

Jianchuan Ancient Town is located in the Jianchuan Basin, surrounded by mountains, and the traffic is not convenient. Compared with other ancient road stations along the Dali Tea Horse Road route, the tourism development of the Jianchuan Ancient Town is lagging behind, retaining more complete ancient architecture. Among them, more than 40 buildings from the Ming Dynasty and 146 buildings from the Qing Dynasty are still preserved, and the rest of them are civil and wooden structures before 1960. In particular, Ximen Street was built between 1500 and 1629, which is a well-preserved, large, and concentrated group of precious historical buildings in Yunnan.

2.2 SAR images and ancillary data

A total of 74 TerraSAR-X images acquired from August 2017 to November 2019 in ascending orbit were used to monitor the Jianchuan Ancient Town. In addition, we also collected a digital orthophoto map (DOM) of Jianchuan Ancient Town in July 2023, with an average ground sampling distance (GSD) of 1.71 cm/0.67 in (Figure 2).
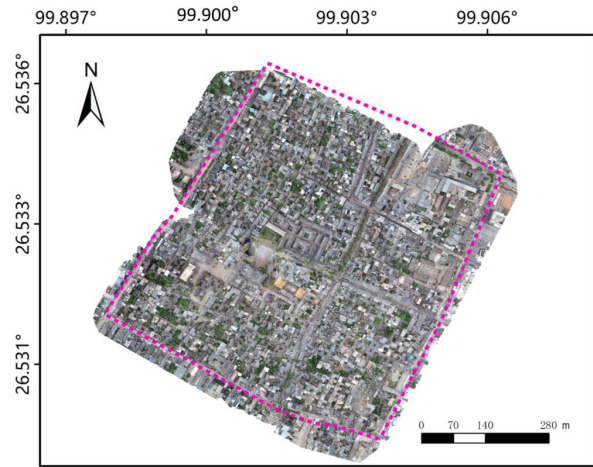

Figure 2. UAV orthophoto of Jianchuan Ancient Town.

Sensor	TerraSAR-X
Wavelength	X
Master	2018/11/02
Time interval	2017/08/30 - 2019/11/22
Number of images	74
Geometry	Ascending
Incidence angle	0.5796

Table 1. Main features of the SAR images used.

3. Methodology

The workflow in this study consists of two parts, as shown in Figure 3. First of all, the surface deformation velocity and time series of the ancient town were estimated based on SBAS-InSAR. In addition, the relationship between LOS deformation and the stability of architectural heritage was analysed by establishing stability evaluation indicators. Then, according to the indicators, the stability level of each heritage was determined.
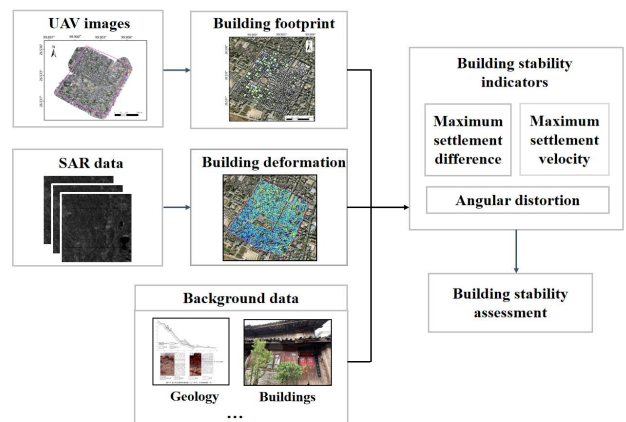

Figure 3. Workflow of methodology.

3.1 Deformation monitoring based on SBAS-InSAR

In this study, we used Small Baseline Subset (SBAS) InSAR to estimate the LOS direction deformation of the study area and its surroundings. SBAS-InSAR is an InSAR time-series technique that provides precise deformation measurements with high spatial density of permanent scatterers (PSs) and effectively

overcomes the spatial decoherence phenomenon. It constructs a series of interferograms with small spatial-temporal baselines and retrieves time-series cumulative deformation using the least-squares method (Usai, 2001). Then, due to rank deficit problems occurring during the least-squares solution process, the singular value decomposition (SVD) algorithm is used to calculate the deformation (Berardino et al., 2002).

Firstly, obtain $N+1$ SAR images covering the study area with ordered time t_1, ..., t_{N+1}. Select one image as the main image and align the other N images to it. N+1 SAR images generate M differential interferograms, and M satisfies:

$$\frac{N+1}{2} \le M \le \frac{N(N+1)}{2} \tag{1}$$

Assuming that the jth interferogram is generated by two SAR images acquired at time t_A and t_B ($t_B > t_A$), the interferometric phase of a pixel with radar coordinates (x, r) of the is expressed as follows:

$$
\begin{aligned}
\delta\phi_j(x,r) &= \phi_B(x,r) - \phi_A(x,r) \\
&\approx \frac{4\pi}{\lambda}[d(t_B,x,r) - d(t_A,x,r)] \\
&\quad + \Delta\phi_{topo}^j + \Delta\phi_{APS}^j + \Delta\phi_{noise}^j
\end{aligned}
\tag{2}
$$

where
$\phi t_A(x, r)$ = the phase of pixel (x, r) at time t_A
$\phi t_B(x, r)$ = the phase of pixel (x, r) at time t_B
$d(t_A, x, r)$ = the LOS cumulative deformation with respect to the reference time t_0 at time t_A
$d(t_B, x, r)$ = the LOS cumulative deformation with respect to the reference time t_0 at time t_B
$\Delta\phi_{topo}^j$ = the topographic phase
$\Delta\phi_{APS}^j$ = the atmospheric phase
$\Delta\phi_{noise}^j$ = the random noise phase

If the phase error component mentioned above is removed, the simplified equation (2) is:

$$\delta\phi_j(x,r) \approx \frac{4\pi}{\lambda}[d(t_B,x,r) - d(t_A,x,r)] \tag{3}$$

Equation (3) produces M equations with N parameters, which are represented by a matrix:

$$A v_{LOS} = \delta\phi \tag{4}$$

where
A = a $M \times N$ coefficient matrix
v_{LOS} = the mean phase velocity vector in the LOS direction

When the interferograms all belong to a single small baseline subset, the least-squares method can be used to calculate the deformation rate:

$$\hat{\phi} = (A^T A)^{-1} A^T \delta\phi \tag{5}$$

If the interferograms belong to two or more subsets, SVD method is used.

In addition, we use generic atmospheric correction online service (GACOS) for InSAR atmospheric delay correction.

GACOS is a method based on numerical weather models that iterates a tropospheric decomposition model to separate stratified and turbulent signals, (Yu et al., 2017).

3.2 Stability indicators

In order to evaluate the structural health of architectural heritage, we combined the surface deformation and the angular distortion to assess the stability of the buildings.

3.2.1 Surface deformation: Based on the deformation velocity of the building surface along the LOS direction, the subsidence velocity is computed by the following equation:

$$\delta_{sub} = \frac{\delta_{LOS}}{\cos\theta} \tag{6}$$

where
δ_{LOS} = LOS deformation velocity
δ_{sub} = subsidence velocity
θ = satellite incidence angle

The maximum differential velocity is characterized as the uneven subsidence on the buildings, which could be calculated as the maximum differential subsidence velocity between two PSs in the building buffer:

$$\Delta_{max} = |\delta_{max} - \delta_{min}| \tag{7}$$

where
δ_{max} = maximum subsidence deformation velocity
δ_{min} = minimum subsidence deformation velocity
Δ_{max} = maximum differential velocity

3.2.2 Angular distortion: Angular distortion is the radian between two PSs, which is related to the measured rotation deformation (Kim et al., 2015). And it is computed by dividing the distance by the arc length that is approximately equal to the differential velocity between the two PSs (Figure 4). Thus, we calculated the maximum angular distortion by using the following equation:

$$\beta = \frac{\Delta_{max}}{L} \tag{8}$$

where
δ_{max} = maximum subsidence deformation velocity
δ_{min} = minimum subsidence deformation velocity
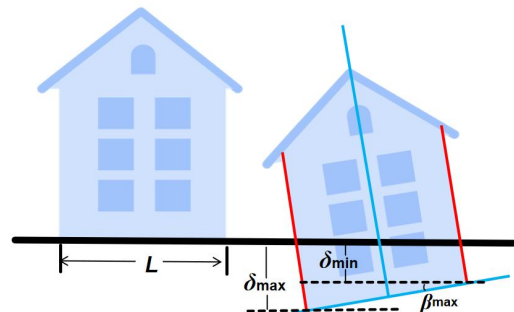Δ_{max} = maximum differential velocity

Figure 4. Schematic representation of indicators.

3.2.3 Architectural heritage stability assessment: Based on InSAR deformation measurements, we developed a building stability level table (Table 2) that shows the above indicators threshold. In Jianchuan Ancient Town, the buildings were categorized into three stability groups: stable, moderate, and unstable. The thresholds for each stability level are set according to (Kim et al., 2015; Ma et al., 2022; Waning, 2014).

Building stability level	Maximum velocity (mm/yr)	Maximum difference (mm/yr)	Angular distortion (rad/yr)
Stable	>-10mm/yr	<10mm/yr	<0.0033
Moderate	Buildings not included in the other level		
Unstable	<-15mm/yr	>15mm/yr	>0.0067

Table 2. The threshold used for stability level classification

4. Results

4.1 Surface deformation rate retrieved by time-series InSAR

We obtained the LOS deformations of PSs in the Jianchuan Ancient Town using the SBAS-InSAR method. Positive velocities indicate deformation towards the satellite, while negative velocities indicate deformation away from the satellite. These velocities may be caused by surface uplift or subsidence. As shown in Figure 5, the deformation velocity of 21822 PSs ranges from -27 to 23 mm/yr. However, most areas of Jianchuan Ancient Town remain stable, with over 93% of the PSs showing a deformation velocity between -5 to 5 mm/yr and over 99% between -10 to 10 mm/yr.
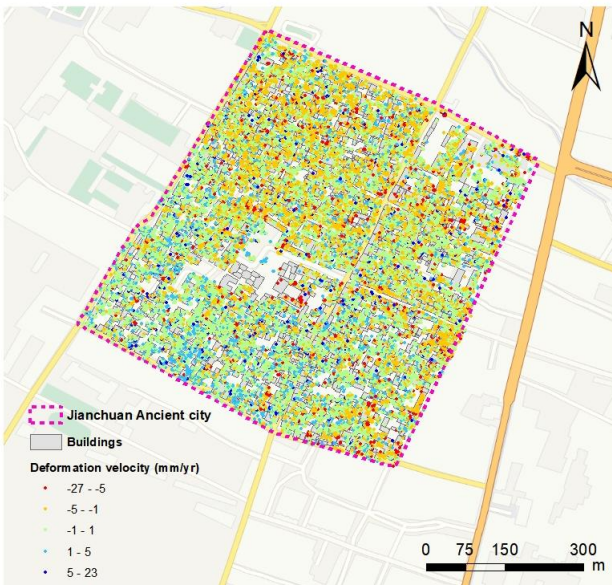

Figure 5. Deformation velocity of PSs in the Jianchuan Ancient Town.

Based on the DSM collected by the UAV, we delineated the footprint of the buildings, and a total of 1891 buildings were delineated. Then, in order to understand and interpret the motion anomalies of the buildings, a buffer zone of 3m was established around each building, and the deformation of PSs within the zone was analysed. The maximum settlement velocity (LOS deformation velocity divided by the cosine of satellite incidence angle) of PSs within the zone determines the maximum subsidence velocity of the building, as shown in

Figure 6. In addition to the maximum subsidence velocity, differences in building subsidence velocity should also be taken into account. To detect and analyse damage, the settlement differential velocity of the building was also calculated for reference, as illustrated in Figure 7. According to the deformation results, we assumed that the building with the maximum subsidence velocity greater than -10mm/yr and the maximum differential velocity smaller than 10mm/yr is stable. Moreover, the building with the maximum subsidence velocity smaller than -15mm/yr and the maximum differential velocity bigger than 15mm/yr is considered unstable.
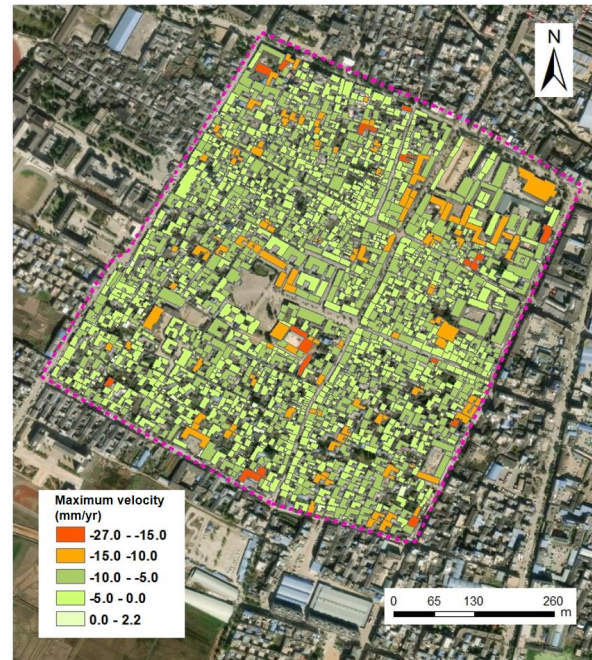

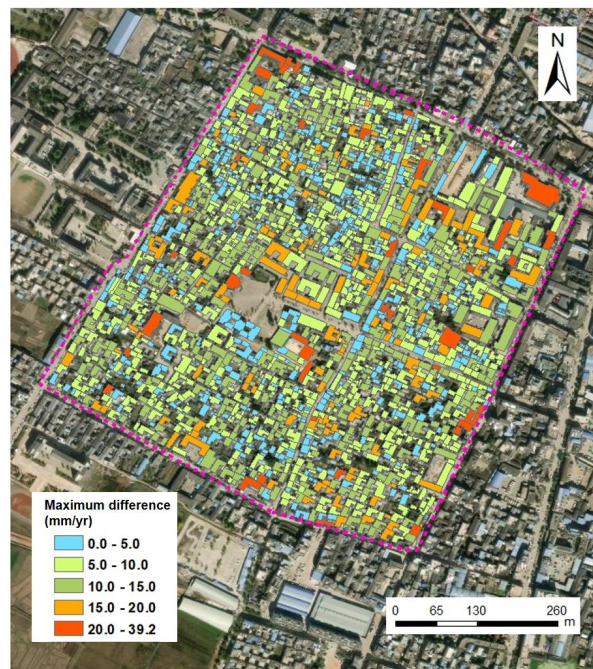Figure 6. Maximum velocity of buildings in the Jianchuan Ancient Town.

Figure 7. Maximum differential velocity of buildings in the Jianchuan Ancient Town.

Nevertheless, relying solely on deformation velocity to evaluate building stability is still insufficient. Therefore, we introduce angular distortion for evaluation. It was recommended that a tolerable threshold of 1/300 be adopted because if the angular distortion exceeds 1/300, visible cracks may appear in the walls, and if it exceeds 1/150, damage to the poles or beams might occur (Gray, 2004). The angular distortion results suggest that the values of most buildings are below the building damage threshold of 0.0033 (Figure 8). In addition to the deformation threshold mentioned above, we include an angle distortion of less than 0.0033 as a criterion for categorizing buildings as stable, and exceeding 0.0067 as a criterion of unstable level. Other buildings that are not assessed as stable or unstable are categorized as moderate.
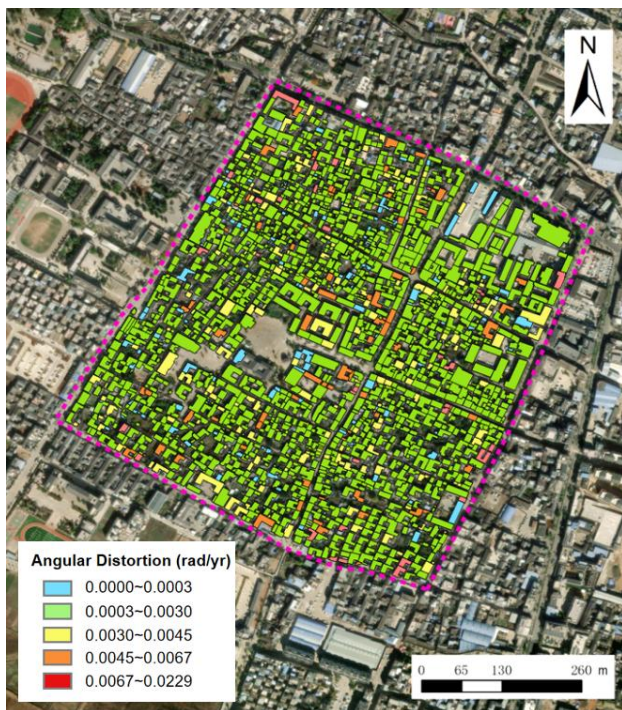

Figure 8. Angular distortion of buildings in the Jianchuan Ancient Town.

4.2 Stability of buildings in Jianchuan Ancient Town

We used the maximum subsidence velocity, the maximum differential deformation, and angular distortion calculated from the TerraSAR-X images to assess the stability of the buildings in the Jianchuan Ancient Town. Our evaluation reveals that out of 1891 buildings in Jianchuan Ancient Town, 1191 and 696 are deemed stable and moderate stability level, respectively (Figure 9a). Buildings with stable level are considered to have almost no deformation, and those with moderate level have negligible deformation and do not pose a threat to stability. As a result, over 99% of the buildings in the Jianchuan Ancient Town are believed to be in good condition. However, four buildings are rated at unstable level, signifying instability and necessitating specific maintenance activities, constituting approximately 0.002% of the total buildings.

In order to further observe these four unstable buildings, we analysed their deformation time series information. The time-series analysis of deformation reveals that Buildings B and D experienced deformation velocities ranging from -5 to 5 mm/yr, with no significant trend. However, the deformation of Building

C exhibited an accelerating trend, reaching -10 mm/yr in April 2018, followed by fluctuations between -12 mm/yr. Building A, in particular, shows a severe accelerating trend, with deformation fluctuating above and below -5mm/yr before August 2018, while showing a significant accelerating after that, even reaching a deformation of -31.4mm/yr (Figure 9b). Based on the above analysis, Building A poses a high risk of instability, necessitating immediate attention and maintenance.
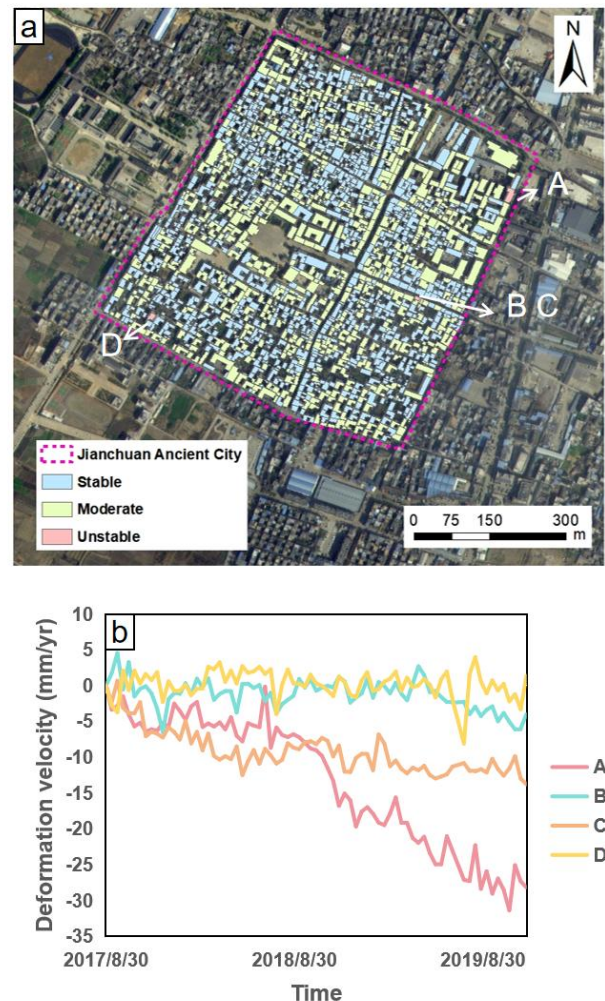

Figure 9. a) Building stability level map in the Jianchuan Ancient Town from 2017 to 2019. b) Deformation time series of four unstable buildings.

5. Conclusion

In this paper, we evaluate the stability of the Jianchuan Ancient Town by analysing the differential deformation and angular distortion of buildings based on InSAR line-of-sight (LOS) deformations. Seventy-four TerraSAR-X images were processed using SBAS-InSAR, yielding deformation velocity and time series results from August 2017 to November 2019. We found that most areas of Jianchuan Ancient Town remain stable, with over 99% of the permanent scatterers (PSs) showing a deformation velocity between -10 to 10 mm/yr. Our evaluation revealed that out of 1891 buildings in Jianchuan Ancient Town, 1191 are deemed stable. Moderate stability is assigned to 696 buildings, denoting minimal deformations with low potential safety hazards. Four buildings are rated as unstable, signifying instability and necessitating specific

maintenance activities. Significantly, one of the unstable buildings showed a severe accelerating trend that require focused attention. The methodology can be applied to other ancient cities and enhance the capability to assess the stability of large-scale architectural heritages.

Although we have expanded the monitoring indicators, there is still some work that needs to be further researched. Firstly, to ensure valid monitoring of building stability, it is necessary to improve the accuracy of InSAR results. Moreover, improving the accuracy of PSs and building positioning is crucial.

Acknowledgements

References

Berardino, P., Fornaro, G., Lanari, R., Sansosti, E., 2002. A new algorithm for surface deformation monitoring based on small baseline differential SAR interferograms. *IEEE Transactions on Geoscience and Remote Sensing* 40, 2375-2383.

Bianchini, S., Pratesi, F., Nolesini, T., Casagli, N., 2015. Building deformation assessment by means of persistent scatterer interferometry analysis on a landslide-affected area: the Volterra (Italy) case study. *Remote Sensing* 7, 4678-4701.

Chen, F., Guo, H., Ishwaran, N., Liu, J., Wang, X., Zhou, W., Tang, P., 2019. Understanding the relationship between the water crisis and sustainability of the Angkor World Heritage site. *Remote Sensing of Environment* 232.

Chen, F., Guo, H., Ma, P., Tang, Y., Wu, F., Zhu, M., Zhou, W., Gao, S., Lin, H., 2023. Sustainable development of World Cultural Heritage sites in China estimated from optical and SAR remotely sensed data. *Remote Sensing of Environment* 298.

Chen, F., Liu, H., Xu, H., Zhou, W., Balz, T., Chen, P., Zhu, X., Lin, H., Fang, C., Parcharidis, I., 2021. Deformation monitoring and thematic mapping of the Badaling Great Wall using very high-resolution interferometric synthetic aperture radar data. International Journal of Applied Earth Observation and Geoinformation 105.

Chen, F., You, J., Tang, P., Zhou, W., Masini, N., Lasaponara, R., 2017. Unique performance of spaceborne SAR remote sensing in cultural heritage applications: overviews and perspectives. *Archaeological Prospection* 25, 71-79.

Chen, F., Zhou, W., Tang, Y., Li, R., Lin, H., Balz, T., Luo, J., Shi, P., Zhu, M., Fang, C., 2022. Remote sensing-based deformation monitoring of pagodas at the Bagan cultural heritage site, Myanmar. *International Journal of Digital Earth* 15, 770-788.

Cigna, F., Balz, T., Tapete, D., Caspari, G., Fu, B., Abballe, M., Jiang, H., 2023. Exploiting satellite SAR for archaeological prospection and heritage site protection. *Geo-spatial Information Science*, 1-26.

Du, Y.-N., Feng, D.-C., Wu, G., 2024. InSAR-based rapid damage assessment of urban building portfolios following the 2023 Turkey earthquake. *International Journal of Disaster Risk Reduction* 103.

Gray, R.M., 2004. Using slab-on-Ground elevation measurements in residential foundation engineering performance evaluations, technical presentation at a meeting of the Houston based Foundation Performance Association, Huston, Texas.

Kim, T.-H., Kim, K.-H., Choi, Y.-C., 2015. Assessment of angular distortion of structures adjacent to a road embankment site. *Measurement* 74, 268-277.

Ma, P., Zheng, Y., Zhang, Z., Wu, Z., Yu, C., 2022. Building risk monitoring and prediction using integrated multi-temporal InSAR and numerical modeling techniques. *International Journal of Applied Earth Observation and Geoinformation* 114.

Nappo, N., Peduto, D., Polcari, M., Livio, F., Ferrario, M.F., Comerci, V., Stramondo, S., Michetti, A.M., 2021. Subsidence in Como historic centre (northern Italy): Assessment of building vulnerability combining hydrogeological and stratigraphic features, Cosmo-SkyMed InSAR and damage data. *International Journal of Disaster Risk Reduction* 56.

Peduto, D., Nicodemo, G., Maccabiani, J., Ferlisi, S., 2017. Multi-scale analysis of settlement-induced building damage using damage surveys and DInSAR data: A case study in The Netherlands. *Engineering Geology* 218, 117-133.

Tang, P., Chen, F., Zhu, X., Zhou, W., 2016. Monitoring cultural heritage sites with advanced multi-Temporal InSAR technique: the case study of the Summer Palace. *Remote Sensing* 8.

Tapete, D., Cigna, F., 2017. InSAR data for geohazard assessment in UNESCO World Heritage sites: state-of-the-art and perspectives in the Copernicus era. *International Journal of Applied Earth Observation and Geoinformation* 63, 24-32.

Usai, S., 2001. A new approach for longterm monitoring of deformations by differential SAR interferometry.

Waning, H.W.v., 2014. A feasibility study of building monitoring and forensic engineering with Interferometric Synthetic Aperture Radar. Delft University of Technology.

Yu, C., Penna, N.T., Li, Z., 2017. Generation of real-time mode high-resolution water vapor fields from GPS observations. *Journal of Geophysical Research: Atmospheres* 122, 2008-2025.

Zhou, W., Chen, F., Guo, H., 2015. Differential Radar Interferometry for Structural and Ground Deformation Monitoring: A New Tool for the Conservation and Sustainability of Cultural Heritage Sites. *Sustainability* 7, 1712-1729.